International Journal of Food Microbiology 304 (2019) 58–67

Contents lists available at ScienceDirect

International Journal of Food Microbiology

journal homepage: www.elsevier.com/locate/ijfoodmicro

Amplification of Raman spectra by gold nanorods combined with chemometrics for rapid classification of four *Pseudomonas*

Shuangshuang Liu, Huanhuan Li, Md Mehedi Hassan, Jiaji Zhu, Ancheng Wang, Qin Ouyang, Muhammad Zareef, Quansheng Chen*

School of Food and Biological Engineering, Jiangsu University, Zhenjiang 212013, PR China

ARTICLE INFO

Keywords:
Surface-enhanced Raman scattering (SERS)
Pseudomonas spp.
Classification
Multivariate calibration

ABSTRACT

This paper demonstrates the application of surface-enhanced Raman scattering (SERS) using positive charged gold nanorods (Au NRs) as an enhancement substrate to classify *Pseudomonas* spp. coupled with multivariate methods. Four species of *Pseudomonas* as dominant spoilage bacteria of food were isolated from rotten chicken, namely, *Pseudomonas gessardii* (P9), *Pseudomonas psychrophila* (P8), *Pseudomonas psychrophila* (S2) and *Pseudomonas fluorescens* (T3). Au NRs were synthesized with positive charge by seed-mediated growth method which can be adsorbed onto the surface of the bacteria by electrostatic adsorption. SERS spectra were collected individually for four types of *Pseudomonas* and pretreated by mean centering (MC), then principal component analysis (PCA) and hierarchical clustering analysis (LDA) were used to achieve data dimensionality reduction and visualize the result of differentiation for the species of *Pseudomonas*. Particularly, the classification accuracy of LDA was reached to 100%. Following we applied hierarchical clustering analysis (HCA) to cluster each species of *Pseudomonas* and the results of HCA consistent with the results of 16S rRNA. This study has shown that SERS combined with LDA and HCA can be used as a reliable method to classify *Pseudomonas*.

1. Introduction

Poultry, the second most consumed meat in the world after pork, is a nutritious and delicious food to human but also ideal medium for the growth of many pathogenic and spoilage bacteria (Silva et al., 2018). Poultry meat is generally kept in frozen condition to prevent its rapid decay. However, previous research has suggested that under lower temperature and aerobically-stored poultry meat can be mainly contaminated by *Pseudomonas* spp. (Dominguez and Schaffner, 2007). *Pseudomonas* spp. are the most common food spoilage bacteria, and can cause spoilage of meat (Cheng et al., 2016; Godziszewska et al., 2017), vegetables (Ioannidis et al., 2018), milk (Yuan et al., 2018), ricotta fresca cheese (Spanu et al., 2018), sausage (Raimondi et al., 2018) and so on. Consequently, several researches are carried out for the construction of mathematical model to predict the shelf life of food items regarding the growth of *Pseudomonas* spp. in an ideal condition (Ghollasi-Mood et al., 2017; Tarlak et al., 2018). However, the growth and metabolic ability of various *Pseudomonas* strains are different which result in diverse spoilage speed of food in the same storage condition. In order to better predict food shelf-life, it is needed to classify and identify *Pseudomonas* strains in a quick and simple way.

Currently, for identification and classification of bacterial strains, physiological, biochemical, serological, chemotaxonomic and genomic methods have been applied in microbiology (Chen et al., 2014). These methods can be categories into three groups: culture-colony counting methods, immunological techniques and polymerase chain reaction (PCR) (Kearns et al., 2017; Pan et al., 2015). However, culture counting techniques involve multiple selective separated cultures as well as several biochemical analyses which are time-consuming and cost intensive (Kutsanedzie et al., 2018). Immunological techniques are comprised of several steps using an active enzyme which needed special storage condition that slows down their real application (Pan et al., 2015). Whereas, PCR requires sophisticated instruments, complicated sample pretreatment as well as expensive reagents (Pan et al., 2015). Therefore, look for a faster, cost-effective and more sensitive way has raised a continued growing interest.

Surface-enhanced Raman scattering (SERS) is an ultrasensitive and selective analytical technique that can be used to detect close proximity analyte based on the enhancement of noble metal nanoparticles (Bozkurt et al., 2018). SERS have the advantages of easy sample preparation, nondestructive, and rapid data acquisition (Li et al., 2017; Wang et al., 2018). However, SERS signals are directly related to the

* Corresponding author.
E-mail address: qschen@ujs.edu.cn (Q. Chen).

https://doi.org/10.1016/j.ijfoodmicro.2019.05.020
Received 5 October 2018; Received in revised form 22 April 2019; Accepted 23 May 2019
Available online 25 May 2019

characteristics of SERS substrate such as size, shape, and distribution of the metal nanostructures which facilitates the better molecular adsorption and sensitive detection of analytes either by an electromagnetic mechanism (EM) or chemical mechanism (CM) (Bharadwaj et al., 2018). Ag and Au nanoparticles are the most common used SERS substrates (Chen et al., 2018; Yang et al., 2017), because they have good performance of exciting localized surface plasmons (LSPs) which can induce strongly enhanced electric fields around the metal nanoparticles (Chen et al., 2017a; Chen et al., 2017b; Chen et al., 2017d; Chen et al., 2016). In recent years, SERS has been shown to be a powerful and promising technology for bacteria differentiation and classification because of its ability to generate entire organism fingerprints (Wang et al., 2018). Gaus et al. (2006) used UV-resonance Raman spectroscopy to identify eight different strains of *lactic acid* bacteria grown on milk-agar with the help of chemometric methods and the 100% classification result was obtained when LDA was used. Anna Muhlig et al. (2016) developed a closed droplet based lab-on-a-chip (LOC) to differentiate *Mycobacterium tuberculosis* complex (MTC) and nontuberculous *mycobacteria* (NTM) using SERS combined with principle components-linear discriminant analysis (PC-LDA), finally, the differentiation accuracy of MTC and NTM was reached to 93.3%. K. Sanna Uusitalo et al. (2017) used AuSi NCs as enhancement substrate to identify three spoilage yeasts and from the SERS spectra they discriminated them at the strain level. Jing Chen et al. (2017c) synthesized PVA-stabilized silver nanoparticles to identify and classify pathogenic bacteria and with the help of PC-LDA and support vector machines (SVM) models they have achieved prediction accuracies from 93% to 100% and from 87% to 100% for detecting *Salmonella* from other species and characterizing the serotypes of *Salmonella* respectively. Although, there are so many researches have been carried out about using SERS technology to differentiate bacteria, but mostly the studies reported on pathogenic bacteria, only few studies are reported on spoilage bacteria and no study reported on *Pseudomonas* yet.

Therefore, the aim of this paper is attempt to use SERS with the help of multivariate analysis to classify four species of *Pseudomonas*. Four *Pseudomonas* strains were isolated from the rotten chicken and the phylogenetic tree was constructed by matching the result of 16S rRNA gene sequencing in Gen Bank. Positively charged Au NRs were fabricated for SERS enhancement, which can easily be adsorbed on the surface of *Pseudomonas* by electrostatic adsorption, enhance the electric fields of the surface of *Pseudomonas* and finally lead to the good SERS spectra of four species of *Pseudomonas*. Unsupervised multivariate methods principal component analysis (PCA), hierarchical clustering analysis (HCA) and supervised classification method linear discriminant analysis (LDA) were introduced after data preprocessed by mean centering (MC) to cluster and discriminate this four relevant *Pseudomonas* species.

2. Materials and methods

2.1. Chemicals

Nutrient agar was purchased from Huankai Microbial Technology Co, Ltd. (Guangdong, China). Cetrimide, fucidin, and cephaloridine (CFC) agar (*Pseudomonas* selective medium) were obtained from Ulva tries biotechnology Co, Ltd. (Shanghai, China). Tryptic soy broth (TSB), cetyltrimethylammonium bromide (CTAB, 99.0%), gold (III) chloride trihydrate ($HAuCl_4$, 99.9%), sodium borohydride ($NaBH_4$, 99.0%), silver nitrate ($AgNO_3$, 99.8%), L-ascorbic acid (AA, 99.0%), hydrochloric acid (HCl, 36%) all the chemicals were purchased from Sinopharm Chemical Reagent Co, Ltd. (Shanghai, China). The fresh breast chicken used in the experiment was purchased from Auchan supermarket meat product counter in Zhenjiang, Jiangsu, China then transported immediately to the laboratory in the sterilized plastic bag and kept in a refrigerator at −18 °C.

2.2. Characterizations

Ultraviolet–visible (UV–Vis) absorption spectra were collected using an 8453 UV–Vis spectroscopy (Agilent Technologies Inc.). The size and morphology of Au NRs were observed by JEM-2100 HR transmission electron microscope (TEM, JEOL Ltd., Japan). The surface charges of Au NRs and four *Pseudomonas* suspensions were measured using Malvern zetasizer Nano ZS90 (Malvern Instruments Ltd., U.K.). Four *Pseudomonas* strains as well as four compounds of *Pseudomonas* and Au NRs were observed by JSF-7800F scanning electron microscopy (SEM, JEOL Ltd., Japan). SERS spectra were collected from a SPLD-RAMAN Spectrometer at 785 nm wavelength incident laser light and 6 cm^{-1} spectral resolution (Hangzhou SPL photonics Co Ltd., China).

2.3. Synthesis of SERS enhancement substrate

Gold nanoparticles were prepared by previous reported seed-mediated growth method (Zheng et al., 2016). For seed solution, 250 μl (0.01 M) $HAuCl_4$ was added to 10 ml (0.1 M) CTAB, then 0.6 ml (0.01 M) ice-cold $NaBH_4$ was introduced to above mixture under vigorous stirring resulting the solution color changed from pale yellow to brown after that the solution was kept at room temperature for 2 h. The growth solution was prepared by sequential addition of 50 ml (0.1 M) CTAB, 0.1 ml (0.01 M) $AgNO_3$, 0.32 ml (0.1 M) AA, 2 ml (0.01 M) $HAuCl_4$, and 0.8 ml (1.0 M) HCl. Finally, 96 μl of as prepared seed solution was added to the above growth solution and stored for 6 h at 27 °C as its color turned into dark blue indicating the large quantity of Au NRs were yielded. The prepared Au NRs were centrifuged at 12,000 rpm for 15 min, washed with water two times and kept the concentrated solution for SERS measurements.

2.4. Screening and purification of spoilage bacteria

10 g rotten chicken was cut into small pieces with sterile scissors and placed in a sterile bottle containing glass beads and 90 ml of saline then sealed and shaken in a shaker at 120 rpm for 30 min. The prepared suspension was diluted to suitable gradients (10^{-6} to 10^{-8} CFU/ml), for each concentration gradient. 100 μl of the bacterial suspension was applied to CFC agar selective medium plate at 37 °C for 48 h. After that, different types of characteristics colonies were selected, separated and plated again to the CFC medium. Thereafter each typical colony was transferred to TSB medium at 37 °C for 12 h for the preservation of different kinds of *Pseudomonas* colonies.

2.5. Biological identification of spoilage bacteria

The typical single colony was used to extract template DNA by heating bacterial suspension in the PCR instrument for 10 min at 100 °C. The universal primers 27 F and 1541R were used to amplify the 16S rRNA strain. The PCR reaction system was constructed by adding 2 μl template DNA, 12.5 μl 2 × PCR mix, 1 μl forward primer 27 F (5′-AGAGTTTGATCCTGGCTCAG-3′), 1 μl reverse primer 1541 R (5′-AAGGAGGTGATCCAGCCGCA-3′) and 8.5 μl sterile water. The PCR parameters were pre-denatured at 95 °C for 5 min followed by 35 cycles at 95 °C for 1 min, 55 °C for 1 min, 72 °C for 1.5 min then an elongation step for 10 min at 72 °C, and finally cooled at 10 °C for 5 min. The amplification products were checked by running 5 μl PCR products on agarose gel electrophoresis at a voltage of 100 V for 30 min (Olsson et al., 2003). The electrophoresis profiles were recorded by gel imaging system and PCR products were sequenced by Gene Company Limited in Beijing. Finally, the phylogenetic tree was constructed by MEGA 5.0 software using more than 99% homology strains that were obtained by matching the sequences with known 16S rRNA sequences in the database of the National Biotechnology Information Center of the United States (http://blast.ncbi.nlm.nih.gov/blast).

2.6. SERS measurements

First, four types of *Pseudomonas* colonies were picked in 25 μl sterile water and mixed with Au NRs colloidal solution thereafter incubated in a shaking table for 3 h at 30 °C with 220 rpm. For each kind of *Pseudomonas* 40 samples were prepared and kept the OD_{600} value of all samples on the range of 0.3–0.5. As a control, we added 25 μl sterile water to Au NRs colloidal solution and relevant SERS spectra was shown in Fig. S1. For collecting SERS spectra, 5 μl of mixed liquid was dripped onto a silicon wafer and illuminated by a 785 nm laser excitation source with the excitation power (360 mW). The SERS spectra were obtained in the wavenumber range of 600 cm^{-1}–1800 cm^{-1}, the integration time was 1 s, and the average scanning rate were 2 times. The laser beam with an approximate diameter of 20 μm spot size was focused onto the SERS measurement zone by a ×50 objective lens, NA = 0.25. Three spectral data were collected from three drops for each bacteria sample and averaged to constitute final spectrum. Finally, a total of 160 spectral data were collected from 160 different samples of four types of *Pseudomonas*.

2.7. Data analysis

In this study, three data preprocess methods namely, standard normal variate transformation (SNV), first derivatives (FD) and mean centering (MC) were comparatively carried out, following the preprocessed data were extracted principal components (PCs) by PCA algorithm respectively and according to the total variance of first three PCs optimized the best data preprocess method. Here, SNV, FD, MC, PCA were performed by MATLAB R2014b (Matworks Inc., Natick, MA, USA). LDA as a supervised classification method was used to achieve excellent classify accuracy of four *Pseudomonas* and further data analysis (Green et al., 2009) and the classification result was performed by leave-one-out tests (Mandrile et al., 2017). HCA was used to cluster each kind of *Pseudomonas* and studied the genetic relationship among the four types of *Pseudomonas*. Here, HCA and LDA were produced by SPSS 16.0 (SPSS Inc., Chicago, IL, USA).

3. Results and discussion

3.1. Characterization of Au NRs

The UV–Vis absorption spectra of Au NRs exhibited two resonance absorption bands with a longitudinal SPR (LSPR) peak at 520 nm and a transverse one at 580 nm shown in Fig. 1A. As CTAB has been used to make Au NRs, the LSPR peak of Au red shifted about 60 nm (Nikoobakht and El-Sayed, 2003). The morphology of Au NRs was confirmed by the TEM image (Fig. 1B) and revealed that the particles were short rod-shaped with an average diameter of 13 ± 3 nm in width, 26.5 ± 6 nm in length. According to previous research, Ag^+ can assist the seed elongation with its ability to induce monolayer formation, and the content of Ag^+ will affect the aspect ratio of Au NRs (Nikoobakht and El-Sayed, 2003). Zeta potential of the dispersed Au NRs was +18.0 mV shown by Fig. 1C, the reason of Au NRs with positive charge is that the Au NRs solution was stabilized by cationic surfactant of CTAB (Ye et al., 2013). As the analytical enhancement factor (AEF) is a pivotal parameter of SERS detection, consequently, the AEF for Au NRs was calculated using the below formula and procedure of reported literature (Hassan et al., 2019). The calculated value of AEF was 8.23×10^6 obtained using the peak at 1613 cm^{-1} of CV. Equal volume of Au NRs and CV with different concentration were used to acquire spectrum for AEF calculation. The Raman and SERS spectrum of CV and the detail calculation of AEF are shown in Fig. S2 and Table S1, respectively.

$$AEF = (I_{SERS}/I_{RS}) \times (C_{RS}/C_{SERS})$$

where C_{RS} is the concentration of an analyte that produces a spontaneous Raman signal I_{RS}, and C_{SERS} is the concentration of same analyte on a SERS substrate which generates SERS signal I_{SERS}.

3.2. Interaction of Au NR and Pseudomonas

Four kinds of *Pseudomonas* were negatively charged confirmed by zeta potential value as exhibited in Fig. 2. Hence, the Au NRs can easily be adsorbed on the surface of *Pseudomonas* by electrostatically. Moreover, the adsorption of Au NRs on the surface of four types of *Pseudomonas* was studied by SEM imaging. The SEM images of four types of *Pseudomonas* were captured in Fig. 3A, B, C and D revealed that the structure of four types of *Pseudomonas* were not raptured by aseptic water within 3–4 h; Fig. 3E–H in the presence of Au NRs showed that four types of *Pseudomonas* were larger in size compared with Au NRs resulting in Au NRs were adsorbed on the surface of *Pseudomonas* and the adsorption was irregular. In addition, it was found from Fig. 3D, H that the surface of *P. fluorescens* may have a layer of capsule which influenced the adsorption of Au NRs with bacteria.

The interaction between Au NRs and four types of *Pseudomonas* were also investigated by UV–Vis spectroscopy. The UV–Vis absorption spectrum of four types of *Pseudomonas* were captured in Fig. 4A. Fig. 4B showed that the peak intensity at 530 nm of Au NRs was decreased and the peak at 585 nm was disappeared when Au NRs adsorbed on four types of *Pseudomonas*. In addition, *P. gessardii* (P9) and *P. fragi* (S2) exhibited a broad peak at around 655 nm and 730 nm respectively and *P. psychrophila* (P8) generated an absorption peak at 650 nm but no new peak was observed for *P. fluorescens* (T3) after interaction with Au NRs.

3.3. SERS spectra of four Pseudomonas

Due to the spontaneous Raman spectra of four kinds of *Pseudomonas* not contained notable peaks, as shown in black lines from Fig. 5, therefore, positive Au NRs was used to enhance the Raman signal of four species *Pseudomonas*. The mean SERS spectra, standard deviation spectra of four types of bacteria were found from the blue lines and red lines respectively of Fig. 5. The dominant SERS peaks of each *Pseudomonas* were noted by red *. We can find that the characteristic peaks of *P. gessardii* (P9) occurred at 758, 821, 951, 1072, 1125, 1140, 1264, 1377, 1447, 1488 and 1572 cm^{-1}; *P. psychrophila* (P8) occurred at 884, 962, 999, 1072, 1140, 1178, 1264, 1340, 1377, 1447, 1492 and 1572 cm^{-1}; *P. fragi* (S2) exhibited SERS typical peaks at 758, 842, 946, 1072, 1140, 1264, 1338, 1377, 1445, 1492 and 1567 cm^{-1}; the typical SERS peaks of *P. fluorescens* (T3) occurred at 966, 1073, 1140, 1264, 1348, 1447, and 1495 cm^{-1}. Those peaks were corresponded to the peaks of cytosine, uracil (758 cm^{-1}), phenylalanine (999 cm^{-1}) and adenine, guanine (1567, 1572 cm^{-1}) (Witkowska et al., 2017), deoxyribose (884 cm^{-1}) (Mungroo et al., 2016), nucleic acids (821, 1338, 1340 and 1348 cm^{-1}), amide III (1264 cm^{-1}) and unsaturated fatty acids (1140 cm^{-1}) (Laucks et al., 2005), carbohydrates (1072 cm^{-1}) (Wang et al., 2010), CH_2 bend of protein, lipid (1426 cm^{-1}) (Uusitalo et al., 2017). Besides, the relevant details were exhibited by Table 1.

The SERS spectra of four types *Pseudomonas* are similar, specifically, the most dominant peak occurs at 1264 cm^{-1} and others peaks at 1072, 1140, 1447 and 1492 cm^{-1}, this is because the cell walls of *Pseudomonas* have similar components, like amino acids, unsaturated fatty acids and amide III etc. However, some differences are evident when comparing the four types of *Pseudomonas* SERS spectra in Fig. 5. In particular, the peaks at 820, 842, 1072, 1445 cm^{-1} in the *P. fragi* (S2) spectra are either not present or are much reduced in the other *Pseudomonas* spectra, the peaks at 884, 999, 1426 cm^{-1} in the *P. psychrophila* (P8) are stronger than other *Pseudomonas* spectra, the peak at 1125 cm^{-1} just exist in *P. gessardii* (P9) spectra. Meanwhile, the SERS intensity and number of all the peaks of *P. fluorescens* (T3) are smallest in four *Pseudomonas* spectra. This may be due to the adsorption of *P. fluorescens* and Au NRs colloid was weaker than that of other *Pseudomonas* species and Au NRs colloid. In addition, the higher the intensity

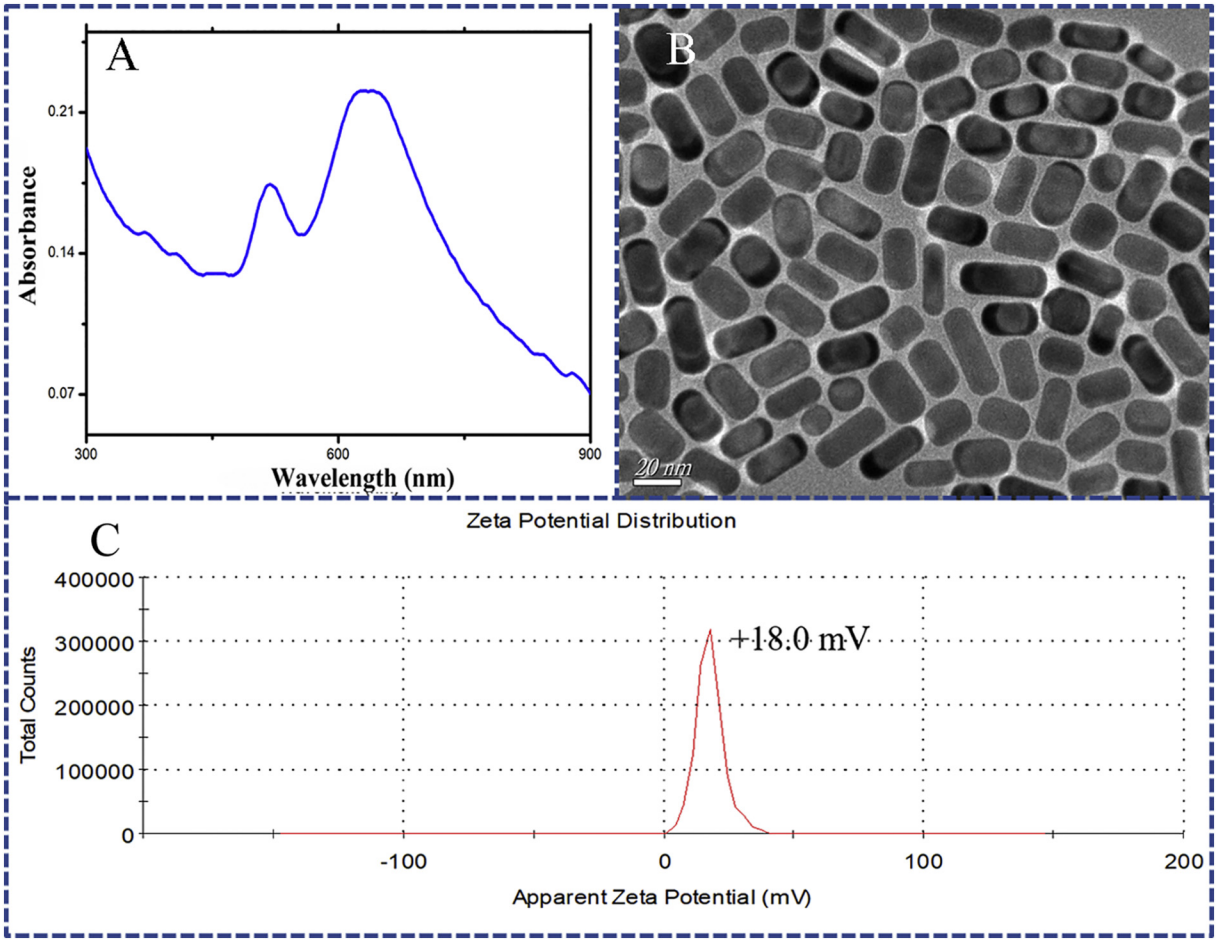

Fig. 1. UV–Vis absorption peak (A), image of transmission electron microscopy (B) and zeta potential value (C) of Au NRs.

of SERS spectra of bacteria, the greater the standard deviation as shown from Fig. 5, since the adsorption of bacteria and Au NRs is spontaneous and irregular which result in adsorption difference of bacteria and Au NRs in different samples and the difference of SERS intensity within same species. The above results indicated that the SERS spectra of bacteria not only related to the compositions of cell wall but also be connected with combination of bacteria and enhancement substrate.

3.4. Results of data dimension reduction and classification

One SERS spectra contained hundreds of variables, which not only contained the nature information of analyte but also contained some useless information like background noise and baseline drift of instrument. Therefore, data preprocessing is needed in order to reduce noise inference (Jaafreh et al., 2018) and data dimensionality reduction is also necessary for eliminate useless information (Muhlig et al., 2016). In this study, we comparatively used three preprocess methods namely SNV, FD and MC. Subsequently PCA was applied to optimize data preprocess method and visualization the differentiation of *Pseudomonas* samples. LDA was used to achieve a satisfactory classification result, a better data dimension reduction and an important information analysis.

PCA is a linear, unsupervised visualization technique used for analyzing and reducing the dimensionality of numerical data sets in a multivariate problem (Khulal et al., 2016). It uses an orthogonal transformation to convert possibly correlated spectral data into few linearly uncorrelated variables, namely principal components (PCs) that retained the information contained in the original spectra (Krahmer et al., 2015). In this work, the data pretreated by three different preprocessed methods separately before PCA, and chose the MC pretreatment due to its highest variance contribution rate of the first three PCs. Table 2 showed the specific variances and total variances of first three PCs performed by three preprocess methods, and the total variances of first three PCs of mean centered-principal components analysis (MC-PCA) was 99.6%, better than first derivatives-principal components analysis (FD-PCA, 99.0%) and standard normal variate transformation-principal components analysis (SNV-PCA, 98.0%). Specially, Table S2 showed the variances and total variances of first ten PCs from MC-PCA, and the variances of PC1, PC2 and PC3 among them were 96.9%, 1.8%, 0.9% respectively. Hence, the first three PCs of MC-PCA were selected, since accounted for 99.6% of total variances in SERS data and were used to construct 3-D scatter plots for visualizing the result of differentiation four types of bacteria. Although the total variances of the first three PCs is over 99%, there are still some overlaps found in scatter plots, for instance, the scatter plots of *P. gessardii* and *P. psychrophila* (P8) are very close, even some overlaps, because the position and intensity of the characteristic peaks in SERS spectra of *P. gessardii* (P9) and *P. psychrophila* (P8) are nearly similar, which can be proved by Fig. 5. In addition, the scatter plots of *Pseudomonas* are too dispersive and the trend of clustering is not ideal, which may attribute to three reasons: firstly, the data used for PCA were full SERS spectra and which also had some useless information; secondly, it may due to the change of SERS peak intensity caused by the uneven adsorption of the bacteria and Au NRs which be observed from Fig. 3; thirdly, PCA only selected first three principle variables from the pretreated data based on variance contribution and other PCs were ignored though that they may bear some important characteristics of bacteria. Hence, it is necessary to apply another data dimension reduction tool which can extract more complete information from pretreated SERS data to

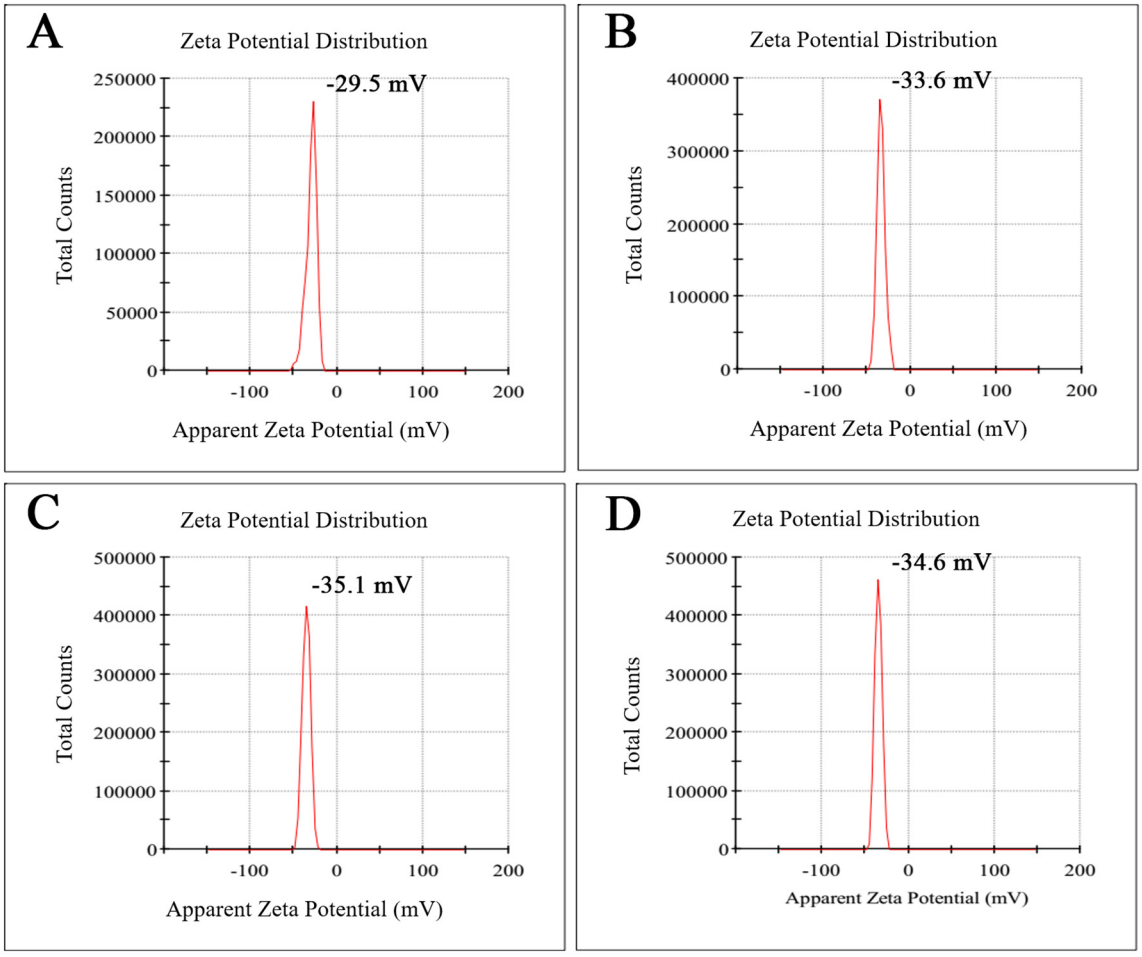

Fig. 2. Zeta potentials of four *Pseudomonas*, *P. gessardii* (A), *P. psychrophila* (B), *P. fragi* (C) and *P. fluorescens* (D).

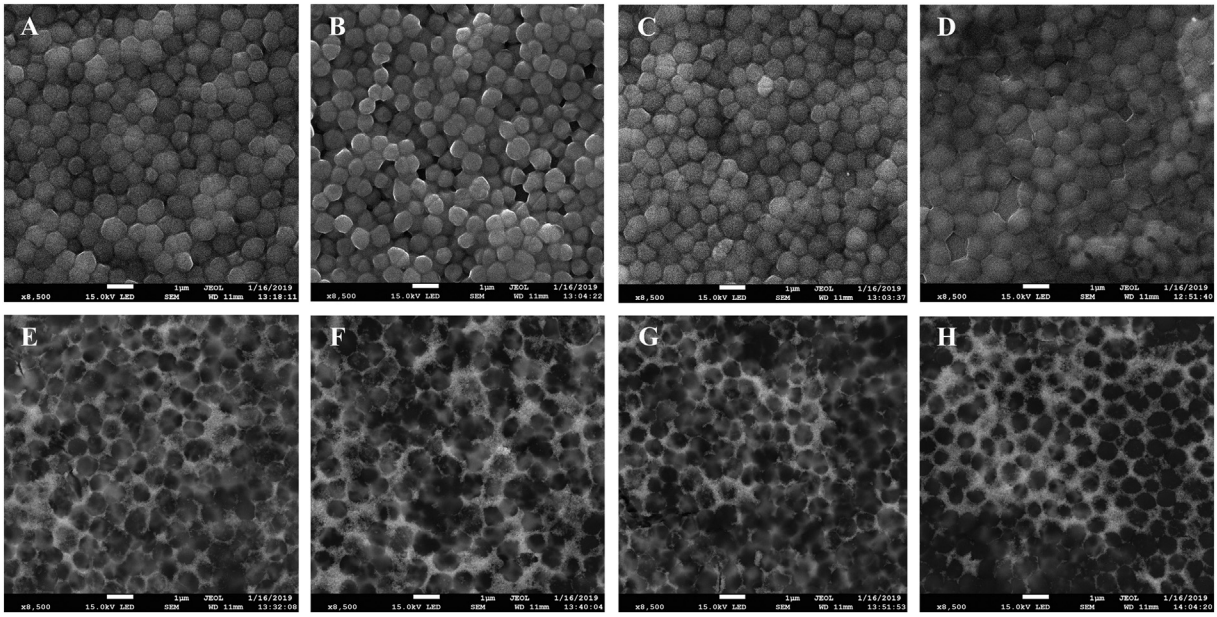

Fig. 3. SEM images of *P. gessardii* (A), *P. psychrophila* (B), *P. fragi* (C), *P. fluorescens* (D) after adsorbed with Au NRs (E), (F), (G) and (H) respectively.

classify bacteria.

LDA is a supervised linear chemometric algorithm that maximizes between groups variances and minimizes within groups variances in order to achieve sample classification (Chen et al., 2014). In this study, LDA was performed to calculate three discriminant functions (DFs) namely DF1, DF2, and DF3 from the data after MC preprocessed using the stepwise method. Table 3 have shown 15 variables selected from original 631 variables by LDA strategy and the values of three DFs

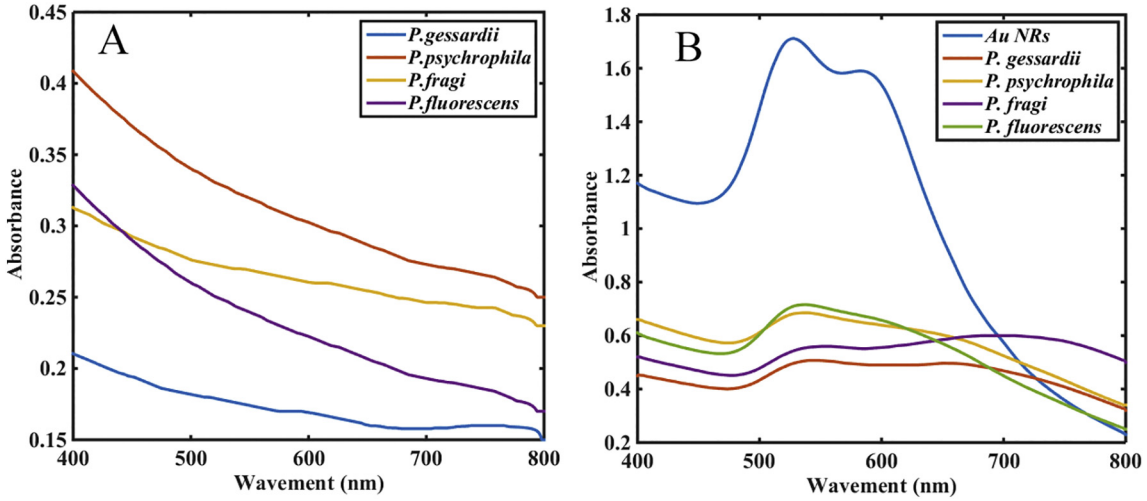

Fig. 4. UV–Vis absorbance spectra of *Pseudomonas* before (A) and after (B) combined with Au NRs.

correspondingly as well as its corresponding Raman assignments. From Table 3, we can find the main contribution for classifying four *Pseudomonas* were from nucleic acids at 780 cm^{-1} (Mungroo et al., 2016), C—C stretching at 842 cm^{-1} and 1125 cm^{-1} (Luo and Lin, 2008; Mungroo et al., 2016), amide I, III, II at 1249, 1271, 1348, 1366, 1368, 1505 and 1509 cm^{-1} (Wang et al., 2010; Witkowska et al., 2017), C—H deformation at 1384, 1415 and 1492 cm^{-1} (Mungroo et al., 2016; Wang et al., 2010). Hence, the major differences of bacteria come from different amide types, C—H deformation and C—C stretching, this result consistent with previous studies (Colnita et al., 2017; Lorenz et al., 2017). To visualize the classification result of LDA, three DFs were used to construct 3-D scatter plots similar to PCA as shown in Fig. 6B. Where, DF1 accounted for 79.4% variances, DF2 produced 13.2% variances and DF3 yielded 7.4% variances. The cumulative variance of three discriminant functions was 100%. Besides, four kinds of *Pseudomonas* were completely distinguished, and different samples of each *Pseudomonas* are clustered in a relatively small area. Moreover, for assessing the performance of the LDA model in terms of general accuracy, leave-one-out cross-validation was employed and the sensitivity and specificity of each *Pseudomonas* species were calculated (Ali et al., 2018; Gaus

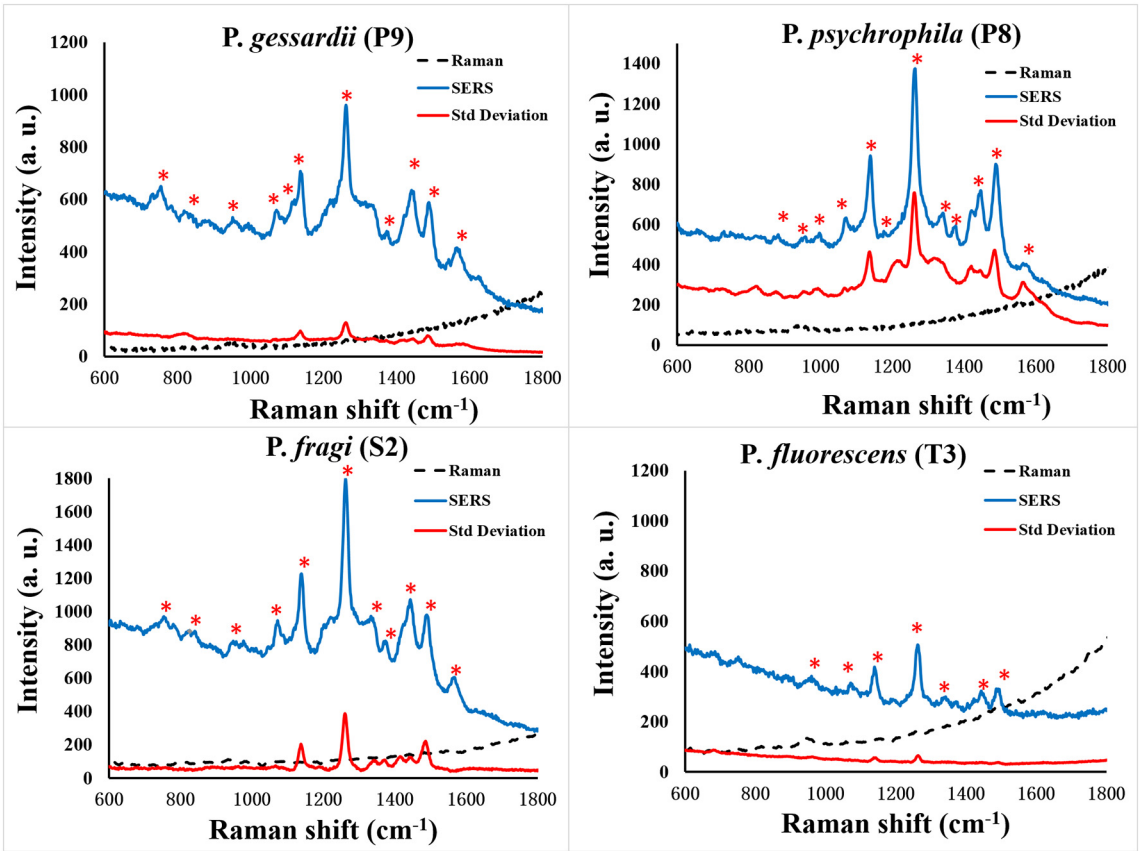

Fig. 5. Mean and standard deviation of replicated SERS spectra of each bacterial type (black lines are the Raman signals of each *Pseudomonas* correspondingly, blue lines are the mean SERS spectra of four *Pseudomonas* separately and the significant peaks was noted by *, red lines are standard deviation calculated form forty SERS spectra for each species of *Pseudomonas*). (For interpretation of the references to color in this figure legend, the reader is referred to the web version of this article.)

Table 1
Tentative assignment of peaks from the SERS spectral of *P. gessardii*, *P. psychrophila*, *P. fragi* and *P. fluorescens*.

Raman shift (cm^{-1})				Assignments
P. gessardii	*P. psychrophila*	*P. fragi*	*P. fluorescens*	
758		758		Cytosine, uracil
821		820		Nucleic acids
		842		Different C–N stretch
	884			Phosphodiester backbone, deoxyribose
951	962	946	966	C=C deformation, C–N stretching
	999			Phenylalanine
1072	1072	1072	1073	Carbohydrates
1125				C–N and C–C stretching/ tryptophan
1140	1140	1140	1140	Unsaturated fatty acids
	1178			15-Methylpalmitic acid
1264	1264	1264	1264	Amide III (random)
	1340	1338	1348	Nucleic acids
1377	1377	1377		Adenine, C–H deformation
	1426			CH_2 bend (protein, lipid)
1447	1447	1445	1447	CH_2 deformation
1492	1492	1492	1495	C–H deformation (lipids)
1572	1572	1567		Adenine, guanine

Table 2
The variances and total variances of first three PCs after preprocessed by different method.

Preprocess methods	Quality index	Principal components		
		PC1	PC2	PC3
SNV	Variances (%)	74.1	19.8	2.1
	Total variances (%)	74.1	93.9	98.0
FD	Variances (%)	93.9	3.3	1.8
	Total variances (%)	93.9	97.2	99.0
MC	Variances (%)	96.9	1.8	0.9
	Total variances (%)	96.9	98.7	99.6

SNV: standard normal variate, FD: first derivatives, MC: mean centering.

et al., 2006; Muhlig et al., 2016; Rodriguez et al., 2013). Here, the sensitivity of each *Pseudomonas* class (corresponding to the proportion of samples in a class that was accurately classified) was 100%, and the specificity of each *Pseudomonas* class (consistent with the proportion of samples classified as a certain class which belong to that class) was also 100%. The classification results of LDA model and leave-one-out cross-validation are shown in Table S3. These results indicated that SERS combined with LDA model could be deployed as a stable and reliable method for the identification of *Pseudomonas* spp.

Compared with PCA, LDA method can take into consideration the class information, minimize the difference of same strains and maximize the difference of different strains (Xu et al., 2016). Despite SERS signals instability in some cases, the results of different bacteria species in PCA and LDA confirmed the ability Au NRs enhanced Raman peaks to differentiate different species of *Pseudomonas*. Especially, when the SERS data was analyzed with LDA, satisfactory classification result was observed.

3.5. Cluster analysis results

In accordance to the above analysis, it was obvious that SERS spectra can be used to distinguish four kinds of *Pseudomonas*. Therefore, we would like to see that whether SERS spectra combined with HCA can be applied to cluster each species of *Pseudomonas* and judge the distance of relationship among four species of *Pseudomonas*. Consequently, the DNA of four sorts of *Pseudomonas* was extracted to get 16S rRNA gene sequence, which was used to construct a phylogenetic tree as a reference standard. Four strains of *Pseudomonas* (P8, S2, T3, and P9) were identified as *P. psychrophila*, *P. fragi*, *P. fluorescens* and *P. gessardii* respectively. Moreover, *P. psychrophila* and *P. fragi* belong to *P. putida* strain, *P. fluorescens* and *P. gessardii* belong to *P. cedrina* strain as shown in Fig. 7B.

HCA classification is based on the Euclidean distance between data elements in their full dimensionality, and the result of HCA is a dendrogram that quantitatively compares the Euclidean distances among all the analyzed data (Suslick et al., 2010). In order to reduce the redundancy of data, forty representative SERS spectra from forty different samples after treated by mean centered-linear discriminate analysis (MC-LDA) were used to generate the clustering of each class by HCA. Fig. 8 showed the ten samples of each *Pseudomonas* strain were accurately identified with no error or misclassifications of 40 cases. Remarkably, the distances of *P. fragi* (S2) and *P. psychrophila* (P8) were adjacent, and the distances of *P. fluorescens* (T3) and *P. gessardii* (P9) were adjacent, which agreed with the result of 16S rRNA gene sequence. Due to the surfaces of bacteria contained different biomolecules originating from the phenotypic character of *Pseudomonas* which is dependent on their genetic structure. Thus the higher homology of genes confer the closer biological molecules on the bacterial surface which shows the more similar SERS spectra that results in closer the Ehrlich distance when HCA is treated. This is why the result of SERS coupled HCA for clustering *Pseudomonas* was in agreement with the genetic relationship of these *Pseudomonas*. For the prospect, as the

Table 3
Selected variables and discriminant functions by LDA based on stepwise method.

Variables	Weight coefficients of discriminant functions			Raman shift (cm^{-1})	Assignments
	DF1	DF2	DF3		
V081	5.924	3.462	9.818	780	Cytosine or uracil (nucleic acids)
V110	−4.959	−0.675	−6.748	842	ν(C–C) in 1,4 glycosidic link
V248	7.267	−8.557	8.926	1125	C–N and C–C stretching/tryptophan
V275	3.595	−5.352	−10.524	1178	15-Methylpalmitic acid
V312	−3.848	4.166	4.497	1249	Amide I
V324	−17.937	10.789	−13.843	1273	Amide III
V365	15.132	−3.227	8.075	1348	Nucleic acids
V375	−13.158	8.092	8.527	1366	=CH in plane (lipid) or amide III (protein)
V376	−15.137	1.020	−5.120	1368	
V385	−9.182	−2.910	1.100	1385	Adenine, C–H deformation
V402	19.617	−5.355	−9.108	1415	CH_2 deformation
V416	0.833	−12.626	4.585	1440	COO^- stretching
V445	13.486	5.614	7.294	1492	C–H deformation (lipids)
V453	−5.693	−10.174	3.983	1506	Amide II
V455	−5.760	−4.921	−14.778	1509	

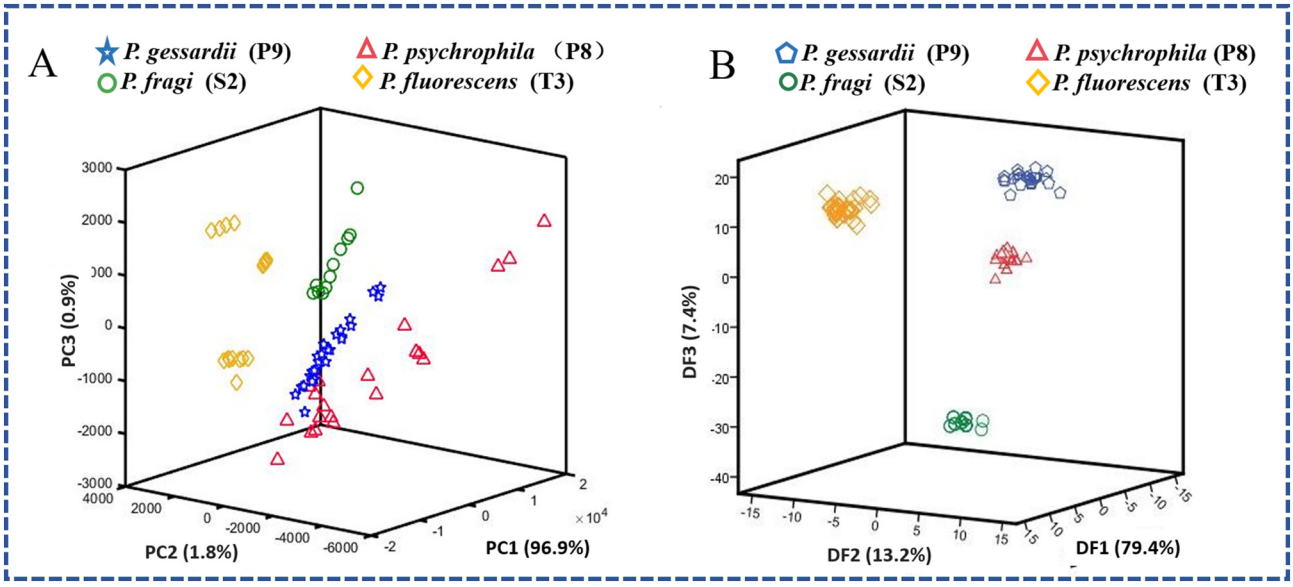

Fig. 6. 3-D scatter plots after data dimension reduction, constructed by selected first three principal components calculated from PCA algorithm (A), constructed by three discriminant functions obtained from LDA analysis (B).

previous study suggested, such clustering analysis is created as for a library of SERS spectra of bacteria, the close genetic relationship of new bacteria can be quantitatively compared to the existing library record, the SERS spectra can tell us what the unknown is "like" (Suslick et al., 2010).

4. Conclusion

In this study, a simple, rapid and sensitive method has been developed to classify four types of *Pseudomonas* isolated from rotten chicken. At first, a stable, positive charged Au NRs as an enhancement substrate was synthesized successfully by seed-mediated growth method and four types of *Pseudomonas* were isolated from rotten chicken. Then, the spectral information of the four spoilage bacteria was successfully collected from the complexes formed by the electrostatic adsorption of bacteria and Au NRs. After that, MC was used to pretreat the SERS data, PCA and LDA were applied to differentiate four types of *Pseudomonas* and LDA achieved 100% discriminant rate during classification. Meanwhile, HCA not only realized the cluster analysis of four kinds of *Pseudomonas*, but also used to judge their genetic relationship, and the result was consistent with the result of 16S rRNA.

Declaration of Competing Interest

All authors declare that they have no conflict of interest.

Acknowledgments

This work has been financially supported by the National Key

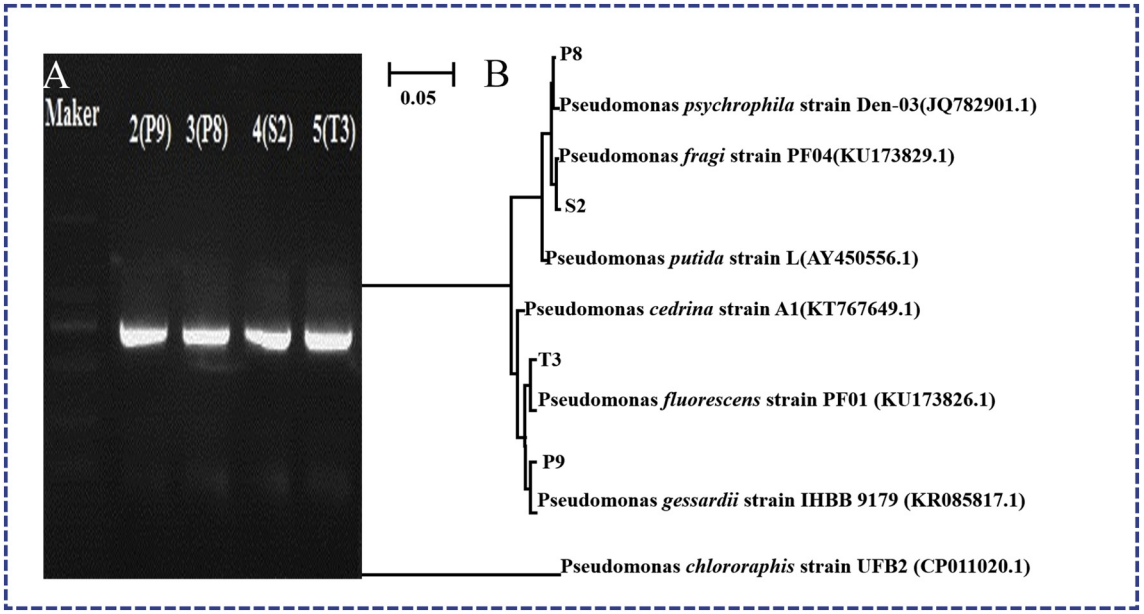

Fig. 7. Electropherogram of PCR amplification products for 16S rRNA genes of the four strains (A), phylogenetic tree of the four strains based on homology of 16S rRNA (B).

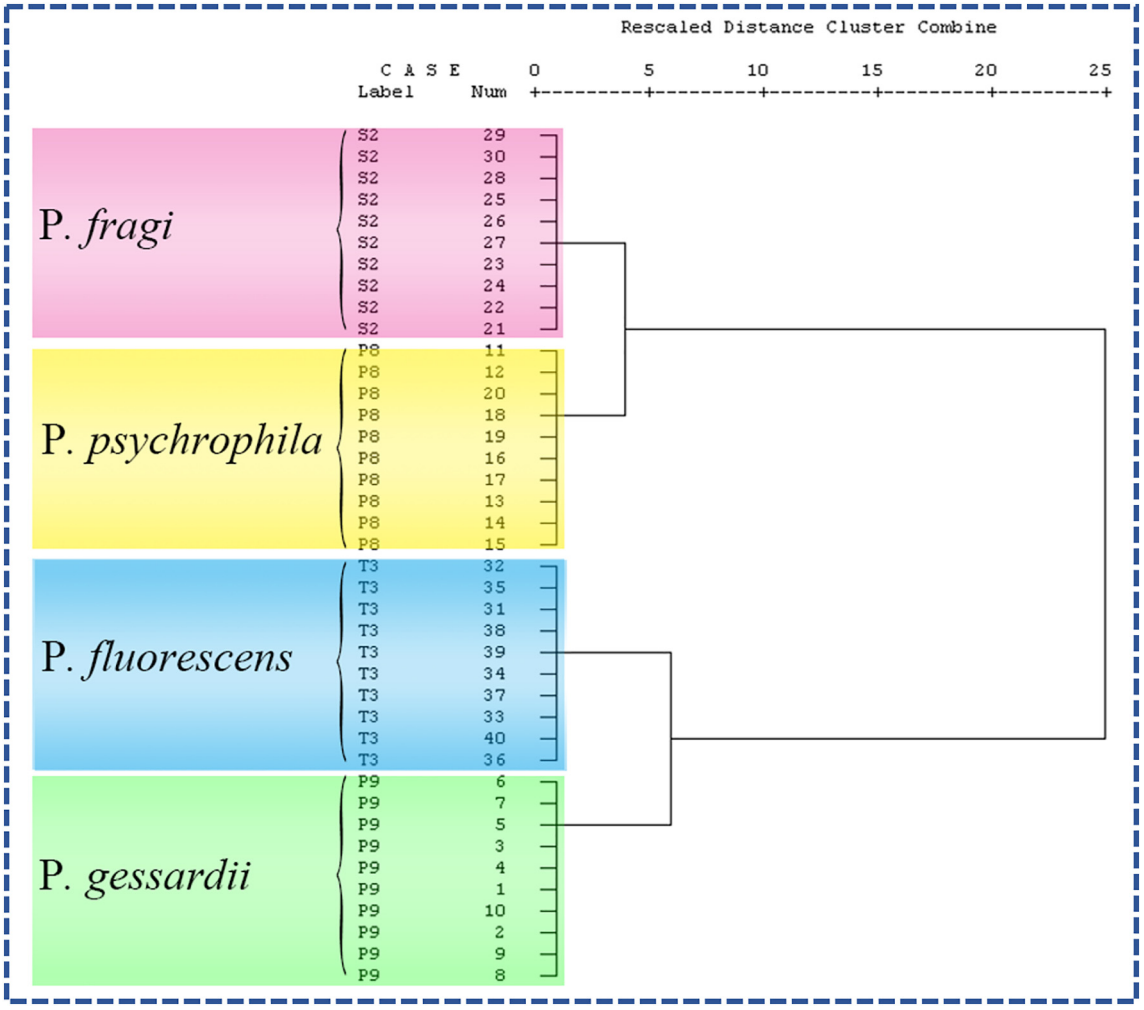

Fig. 8. HCA dendrogram for four *Pseudomonas* strains.

Research and Development Program of China (2016YFD0401205 and 2017YFC1600801). We are also grateful to many of our colleagues for stimulating discussion in this field.

Funding

This study has no financial relationship with organization that sponsored the research.

Ethical approval

This article does not contain any studies with human or animal subjects.

Appendix A. Supplementary data

Supplementary data to this article can be found online at https://doi.org/10.1016/j.ijfoodmicro.2019.05.020.

References

Ali, N., Girnus, S., Rosch, P., Popp, J., Bocklitz, T., 2018. Sample-size planning for multivariate data: a Raman-spectroscopy-based example. Anal. Chem. 90, 12485–12492.
Bharadwaj, S., Pandey, A., Yagci, B., Ozguz, V., Qureshi, A., 2018. Graphene nano-mesh-Ag-ZnO hybrid paper for sensitive SERS sensing and self-cleaning of organic pollutants. Chem. Eng. J. 336, 445–455.
Bozkurt, A.G., Buyukgoz, G.G., Soforoglu, M., Tamer, U., Suludere, Z., Boyaci, I.H., 2018. Alkaline phosphatase labeled SERS active sandwich immunoassay for detection of Escherichia coli. Spectrochim. Acta A Mol. Biomol. Spectrosc. 194, 8–13.
Chen, Q., Li, H., Ouyang, Q., Zhao, J., 2014. Identification of spoilage bacteria using a simple colorimetric sensor array. Sensors Actuators B Chem. 205, 1–8.
Chen, J., Zhang, T., Tang, C., Mao, P., Liu, Y., Yu, Y., Liu, Z., 2016. Optical magnetic field enhancement via coupling magnetic plasmons to optical cavity modes. IEEE Photon. Technol. Lett. 28, 1529–1532.
Chen, J., Fan, W., Mao, P., Tang, C., Liu, Y., Yu, Y., Zhang, L., 2017a. Tailoring plasmon lifetime in suspended nanoantenna arrays for high-performance plasmon sensing. Plasmonics 12, 529–534.
Chen, J., Fan, W., Zhang, T., Tang, C., Chen, X., Wu, J., Li, D., Yu, Y., 2017b. Engineering the magnetic plasmon resonances of metamaterials for high-quality sensing. Opt. Express 25, 3675–3681.
Chen, J., Park, B., Eady, M., 2017c. Simultaneous detection and serotyping of Salmonellae by immunomagnetic separation and label-free surface-enhanced Raman spectroscopy. Food Anal. Methods 10, 3181–3193.
Chen, J., Zha, T., Zhang, T., Tang, C., Yu, Y., Liu, Y., Zhang, L., 2017d. Enhanced magnetic fields at optical frequency by diffraction coupling of magnetic resonances in lifted metamaterials. J. Lightwave Technol. 35, 71–74.
Chen, Q., Yang, M., Yang, X., Li, H., Guo, Z., Rahma, M.H., 2018. A large Raman scattering cross-section molecular embedded SERS aptasensor for ultrasensitive Aflatoxin B1 detection using CS-Fe3O4 for signal enrichment. Spectrochim. Acta A Mol. Biomol. Spectrosc. 189, 147–153.
Cheng, W.W., Sun, D.W., Cheng, J.H., 2016. Pork biogenic amine index (BAI) determination based on chemometric analysis of hyperspectral imaging data. LWT Food Sci. Technol. 73, 13–19.
Colnita, A., Dina, N.E., Leopold, N., Vodnar, D.C., Bogdan, D., Porav, S.A., David, L., 2017. Characterization and discrimination of Gram-positive bacteria using Raman spectroscopy with the aid of principal component analysis. Nanomaterials 7, 16.
Dominguez, S.A., Schaffner, D.W., 2007. Development and validation of a mathematical model to describe the growth of Pseudomonas spp. in raw poultry stored under aerobic conditions. Int. J. Food Microbiol. 120, 287–295.
Gaus, K., Rosch, P., Petry, R., Peschke, K.D., Ronneberger, O., Burkhardt, H., Baumann, K., Popp, J., 2006. Classification of lactic acid bacteria with UV-resonance Raman spectroscopy. Biopolymers 82, 286–290.
Ghollasi-Mood, F., Mohsenzadeh, M., Hoseindokht, M.R., Varidi, M., 2017. Quality

changes of air-packaged chicken meat stored under different temperature conditions and mathematical modelling for predicting the microbial growth and shelf life. J. Food Saf. 37, 9.
Godziszewska, J., Guzek, D., Pogorzelska, E., Brodowska, M., Gorska-Horczyczak, E., Sakowska, A., Wojtasik-Kalinowska, I., Gantner, M., Wierzbicka, A., 2017. A simple method of the detection of pork spoilage caused by Rahnella aquatilis. LWT Food Sci. Technol. 84, 248–255.
Green, G.C., Chan, A.D.C., Luo, B.S., Dan, H., Lin, M., 2009. Identification of Listeria species using a low-cost surface-enhanced Raman scattering system with wavelet-based signal processing. IEEE Trans. Instrum. Meas. 58, 3713–3722.
Hassan, M.M., Chen, Q., Kutsanedzie, F.Y.H., Li, H., Zareef, M., Xu, Y., Yang, M., Agyekum, A.A., 2019. rGO-NS SERS-based coupled chemometric prediction of acetamiprid residue in green tea. J. Food Drug Anal. 27, 145–153.
Ioannidis, A.-G., Kerckhof, F.-M., Riahi Drif, Y., Vanderroost, M., Boon, N., Ragaert, P., De Meulenaer, B., Devlieghere, F., 2018. Characterization of spoilage markers in modified atmosphere packaged iceberg lettuce. Int. J. Food Microbiol. 279, 1–13.
Jaafreh, S., Breuch, R., Gunther, K., Kreyenschmidt, J., Kaul, P., 2018. Rapid poultry spoilage evaluation using portable fiber-optic Raman spectrometer. Food Anal. Methods 11, 2320–2328.
Kearns, H., Goodacre, R., Jamieson, L.E., Graham, D., Faulds, K., 2017. SERS detection of multiple antimicrobial-resistant pathogens using nanosensors. Anal. Chem. 89, 12666–12673.
Khulal, U., Zhao, J.W., Hu, W.W., Chen, Q.S., 2016. Nondestructive quantifying total volatile basic nitrogen (TVB-N) content in chicken using hyperspectral imaging (HSI) technique combined with different data dimension reduction algorithms. Food Chem. 197, 1191–1199.
Krahmer, A., Engel, A., Kadow, D., Ali, N., Umaharan, P., Kroh, L.W., Schulz, H., 2015. Fast and neat - determination of biochemical quality parameters in cocoa using near infrared spectroscopy. Food Chem. 181, 152–159.
Kutsanedzie, F.Y.H., Chen, Q., Hassan, M.M., Yang, M., Sun, H., Rahman, M.H., 2018. Near infrared system coupled chemometric algorithms for enumeration of total fungi count in cocoa beans neat solution. Food Chem. 240, 231–238.
Laucks, M.L., Sengupta, A., Junge, K., Davis, E.J., Swanson, B.D., 2005. Comparison of psychro-active arctic marine bacteria and common mesophillic bacteria using surface-enhanced Raman spectroscopy. Appl. Spectrosc. 59, 1222–1228.
Li, H.H., Chen, Q.S., Hassan, M.M., Chen, X.X., Ouyang, Q., Guo, Z.M., Zhao, J.W., 2017. A magnetite/PMAA nanospheres-targeting SERS aptasensor for tetracycline sensing using mercapto molecules embedded core/shell nanoparticles for signal amplification. Biosens. Bioelectron. 92, 192–199.
Lorenz, B., Wichmann, C., Stockel, S., Rosch, P., Popp, J., 2017. Cultivation-free Raman spectroscopic investigations of bacteria. Trends Microbiol. 25, 413–424.
Luo, B.S., Lin, M., 2008. A portable Raman system for the identification of foodborne pathogenic bacteria. J. Rapid Methods Autom. Microbiol. 16, 238–255.
Mandrile, L., Amato, G., Marchis, D., Martra, G., Rossi, A.M., 2017. Species-specific detection of processed animal proteins in feed by Raman spectroscopy. Food Chem. 229, 268–275.
Muhlig, A., Bocklitz, T., Labugger, I., Dees, S., Henk, S., Richter, E., Andres, S., Merker, M., Stockel, S., Weber, K., Cialla-May, D., Popp, J., 2016. LOC-SERS: a promising closed system for the identification of mycobacteria. Anal. Chem. 88, 7998–8004.
Mungroo, N.A., Oliveira, G., Neethirajan, S., 2016. SERS based point-of-care detection of food-borne pathogens. Microchim. Acta 183, 697–707.
Nikoobakht, B., El-Sayed, M.A., 2003. Preparation and growth mechanism of gold nanorods (NRs) using seed-mediated growth method. Chem. Mater. 15, 1957–1962.
Olsson, C., Ahrne, S., Pettersson, B., Molin, G., 2003. The bacterial flora of fresh and chill-stored pork: analysis by cloning and sequencing of 16S rRNA genes. Int. J. Food Microbiol. 83, 245–252.
Pan, W., Zhao, J., Chen, Q., 2015. Fabricating upconversion fluorescent probes for rapidly sensing foodborne pathogens. J. Agric. Food Chem. 63, 8068–8074.
Raimondi, S., Nappi, M.R., Sirangelo, T.M., Leonardi, A., Amaretti, A., Ulrici, A., Magnani, R., Montanari, C., Tabanelli, G., Gardini, F., Rossi, M., 2018. Bacterial community of industrial raw sausage packaged in modified atmosphere throughout the shelf life. Int. J. Food Microbiol. 280, 78–86.
Rodriguez, S.B., Thornton, M.A., Thornton, R.J., 2013. Raman spectroscopy and chemometrics for identification and strain discrimination of the wine spoilage yeasts Saccharomyces cerevisiae, Zygosaccharomyces bailii, and Brettanomyces bruxellensis. Appl. Environ. Microbiol. 79, 6264–6270.
Silva, F., Domingues, F.C., Nerin, C., 2018. Trends in microbial control techniques for poultry products. Crit. Rev. Food Sci. Nutr. 58, 591–609.
Spanu, C., Piras, F., Mocci, A.M., Nieddu, G., De Santis, E.P.L., Scarano, C., 2018. Use of Carnobacterium spp protective culture in MAP packed Ricotta fresca cheese to control Pseudomonas spp. Food Microbiol. 74, 50–56.
Suslick, B.A., Feng, L., Suslick, K.S., 2010. Discrimination of complex mixtures by a colorimetric sensor array: coffee aromas. Anal. Chem. 82, 2067–2073.
Tarlak, F., Ozdemir, M., Melikoglu, M., 2018. Mathematical modelling of temperature effect on growth kinetics of Pseudomonas spp. on sliced mushroom (Agaricus bisporus). Int. J. Food Microbiol. 266, 274–281.
Uusitalo, S., Popov, A., Ryabchikov, Y.V., Bibikova, O., Alakomi, H.-L., Juvonen, R., Kontturi, V., Siitonen, S., Kabashin, A., Meglinski, I., Hiltunen, J., Laitila, A., 2017. Surface-enhanced Raman spectroscopy for identification and discrimination of beverage spoilage yeasts using patterned substrates and gold nanoparticles. J. Food Eng. 212, 47–54.
Wang, Y.L., Lee, K., Irudayaraj, J., 2010. Silver nanosphere SERS probes for sensitive identification of pathogens. J. Phys. Chem. C 114, 16122–16128.
Wang, C., Gu, B., Liu, Q., Pang, Y., Xiao, R., Wang, S., 2018. Combined use of vancomycin-modified Ag-coated magnetic nanoparticles and secondary enhanced nanoparticles for rapid surface-enhanced Raman scattering detection of bacteria. Int. J. Nanomedicine 13, 1159–1178.
Witkowska, E., Korsak, D., Kowalska, A., Księżopolska-Gocalska, M., Niedziółka-Jönsson, J., Roźniecka, E., Michałowicz, W., Albrycht, P., Podrażka, M., Hołyst, R., Waluk, J., Kamińska, A., 2017. Surface-enhanced Raman spectroscopy introduced into the International Standard Organization (ISO) regulations as an alternative method for detection and identification of pathogens in the food industry. Anal. Bioanal. Chem. 409, 1555–1567.
Xu, L.R., Yu, X.Z., Liu, L., Zhang, R., 2016. A novel method for qualitative analysis of edible oil oxidation using an electronic nose. Food Chem. 202, 229–235.
Yang, M., Liu, G., Mehedi, H.M., Ouyang, Q., Chen, Q., 2017. A universal SERS aptasensor based on DTNB labeled GNTs/Ag core-shell nanotriangle and CS-Fe3O4 magnetic-bead trace detection of Aflatoxin B1. Anal. Chim. Acta 986, 122–130.
Ye, X.C., Zheng, C., Chen, J., Gao, Y.Z., Murray, C.B., 2013. Using binary surfactant mixtures to simultaneously improve the dimensional tunability and monodispersity in the seeded growth of gold nanorods. Nano Lett. 13, 765–771.
Yuan, L., Burmølle, M., Sadiq, F.A., Wang, N., He, G., 2018. Interspecies variation in biofilm-forming capacity of psychrotrophic bacterial isolates from Chinese raw milk. Food Control 91, 47–57.
Zheng, G.C., de Marchi, S., Lopez-Puente, V., Sentosun, K., Polavarapu, L., Perez-Juste, I., Hill, E.H., Bals, S., Liz-Marzan, L.M., Pastoriza-Santos, I., Perez-Juste, J., 2016. Encapsulation of single plasmonic nanoparticles within ZIF-8 and SERS analysis of the MOF flexibility. Small 12, 3935–3943.